

'Electron Temperature and Density Fluctuations
in the Daytime Ionosphere' *

By

J. Doupnik
and
J. S. Nisbet

UNPUBLISHED PRELIMINARY DATA

GPO PRICE \$ _____

CFSTI PRICE(S) \$ _____

Hard copy (HC) 1.00

Microfiche (MF) .50

Ionosphere Research Laboratory
The Pennsylvania State University
University Park, Pennsylvania

ff 653 July 65

Abstract

Large electron temperature fluctuations have been observed in the F region during the day using incoherent scatter measurements at Arecibo. The behavior is quite variable from day to day.

When the fluctuations occur large changes in the equilibrium density distribution result and the electron densities in the layer change rapidly.

The relationship between the electron densities, thermal energies and heat transport rates during these events is discussed.

will be published in revised form

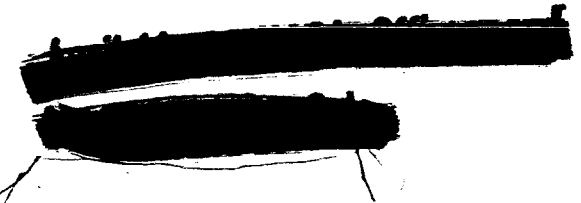
submitted to JGR

author

presented in Norway

FACILITY FORM 802	N66 29347 (ACCESSION NUMBER)	_____ (THRU)
	17 (PAGES)	1 (CODE)
	CR-57304 (NASA CR OR TMX OR AD NUMBER)	13 (CATEGORY)

*The work described in this paper was supported under NASA Grant No. Nsg-134-61, and is based on measurements made in cooperation with the Arecibo Ionospheric Observatory. The Arecibo Ionospheric Observatory is operated by Cornell University with the support of the Advanced Research Projects Agency under a research contract with the Air Force Office of Scientific Research.



1. Observations

In a series of incoherent backscatter measurements at Arecibo, Puerto Rico by Nisbet and Carlson (1965) in the summer and winter of 1964 large fluctuations were noticed in the electron density and temperature. A considerable amount of data ^{were} was obtained in the winter when the magnetic activity was very low and solar conditions were quiet.

One day, December 18, will be considered in detail. Peak electron densities for this day are shown in Figure 1. The major daytime features are a small maximum at 08:15 Hrs. and a large maximum of about twice the normal density centered on 11:00 hrs. In the next two hours, the densities dropped to their normal daytime values. The densities for this figure were computed from Arecibo ionograms.

To examine the consistency of this effect from day to day, Figure 2 shows the maximum electron densities as a function of time for several days within a two week period. It is apparent that though large fluctuations occur on almost all days the times of occurrence are not the same, and that the character changes from one day to another.

The peak electron density alone does not give a good indication of the physical processes occurring in the layer when large movements are present. Figure 3 shows the integrated electron densities up to 460 km obtained from backscatter profiles compared with the peak electron densities shown in the first figure. It is apparent that the electron content of the layer as well as the peak electron density increases by a factor of two around 11:00 when compared to the contents and densities two hours before or after. The irregularities thus do not represent merely a redistribution of ionization. This figure also shows the K_p indices and the decimetric solar flux, both of which indicate no abnormal events.

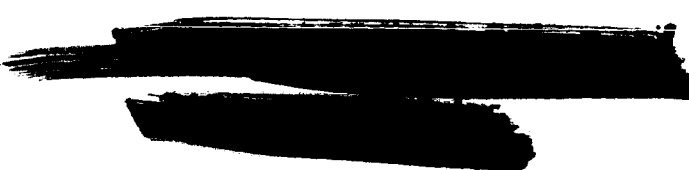


Figure 4 shows electron density height profiles from backscatter measurements throughout this event. On the left hand side of the figure the portion where the electron densities were increasing is shown, and on the right the period when they were decreasing. It is apparent that in the increasing phase of the event the electron densities increase uniformly throughout the layer above 200 km, while below 200 km there is little variation. From 11:00 until noon, the electron density decrease occurs in the region of the maximum and above, the height of the maximum drops, and the densities below the peak increase. From noon until 13 hours the electron density decrease is quite uniform in the region of the peak.

To investigate the behavior below the peak in somewhat greater detail Figure 5 shows the electron densities during the same periods reduced from ionograms using the technique developed by Doupnik and Schmerling (1965). Again, the same general trends are apparent. In the F1 region the electron density increases uniformly throughout the period. The major variations are occurring in the F2 layer. However, it should be noticed that during the decreasing portion of the event the electron densities are larger in the region of 180 km.

Figure 6 shows the observed ion temperatures at several altitudes. Also shown are the neutral temperatures from the Harris and Priester (1962) model for $S_{10.7} = 70$. It is apparent that in the morning and in the late afternoon the neutral temperatures predicted by the models show much slower changes with time than the measured ion temperatures. At 225 km it would be expected that ion and neutral temperatures should follow one another very closely. It would therefore appear that the backscatter spectra can provide useful data on the diurnal variation of the neutral temperatures.

2. Production and Loss in the Layer

To examine the electron density behavior it is first necessary to consider to what extent the observed phenomena agree with what is known about production and loss mechanisms in the layer.

To avoid, to the maximum extent possible, the necessity for considering transport within the layer, the continuity equation was integrated over the height region 140 km to 460 km. Figure 7 shows the integrated continuity equation and the expressions used for the production and loss terms.

Variations of neutral density are important for the examination of loss and production rates. For the present analysis, models due to Harris and Priester (1962) were employed with a first order modification to make the ion and neutral temperatures agree at 225 km.

The loss was assumed to follow ion-atom interchange with molecular nitrogen followed by dissociative recombination. Production was assumed to follow a Chapman distribution. The integrated production was thus independent of the neutral atomic oxygen distribution and dependent on the solar zenith angle. The production was normalized to be equal to the loss at 11:00 a.m. when the rate of change of electron content was zero. No particle flux into or out of the region was assumed.

Figure 8 shows the integrated production and loss during the period from 08:00 to 15:00 hours. It is apparent that during the periods when the electron density was increasing rapidly the calculated production was greater than the calculated loss, and that when the content was decreasing the loss was greater than production. During the afternoon, production and loss were approximately equal.

In Figure 9 are shown the observed rate of change of electron content and that calculated from the difference between integrated production and loss. From 09:00 to 13:00 hours the agreement is quite satisfactory. Outside this period the assumptions made about the neutral atmosphere and the variation of the production function deteriorate.

The observed electron density fluctuations can thus be explained without invoking any sudden increase in production, loss, or electron flux into the observed region.

3. Mechanisms for the Fluctuation

While the preceding analysis has shown that production and loss alone can account for the fluctuations, a mechanism for producing the instability is required.

Figure 10 shows the electron temperatures derived from incoherent backscatter spectra during the day. In the period around 11:00 hours when the electron densities are large, the electron temperatures have a minimum which is very pronounced at 300 km and above. After 11:00 hours when the electron densities are decreasing the electron temperatures increase until 13:00 hours when the layer shape stabilizes.

Figure 11 shows the heat fluxes from electrons to ions during this period calculated using an expression due to Hanson (1963)

$$Q_{ei} = 4.8 \times 10^{-7} N_e^2 \frac{(T_e - T_i)}{T_e^{3/2}} \text{ ev cm}^{-3} \text{ sec}^{-1} .$$

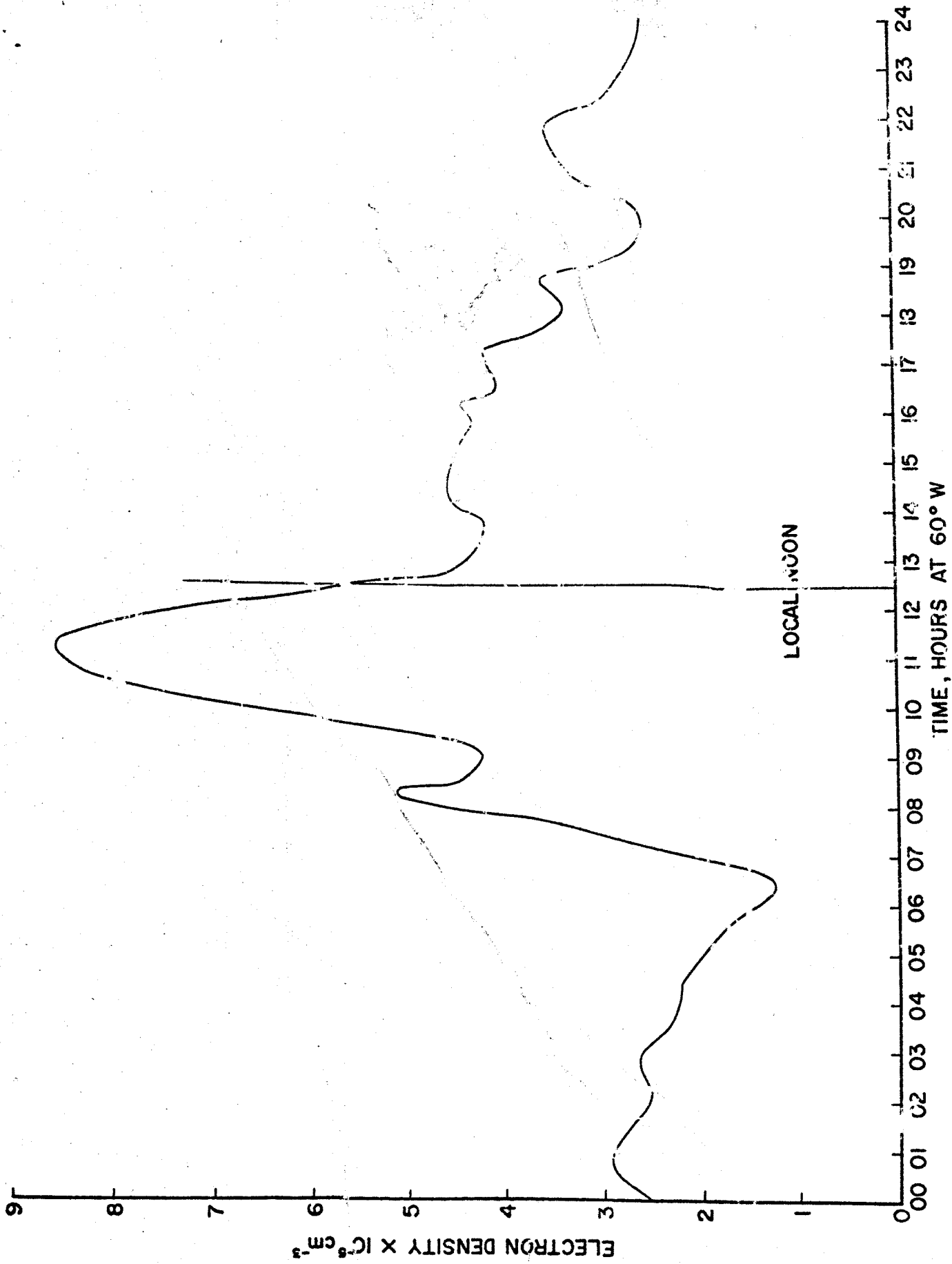
It is postulated that the instability results from the following process. A small increase in electron density in the region of the peak will increase the rate of heat transfer from electrons to ions, reducing the electron

temperature, and hence the plasma scale height. Downward diffusion will follow to equalize the distribution, thus further increasing the heat transport and reducing the scale heights.

The mechanism for the initiation of the events can only be hypothesized at present, but there does seem to be a correlation between the time at which the electron densities start to increase and the ion temperatures on the preceding night.

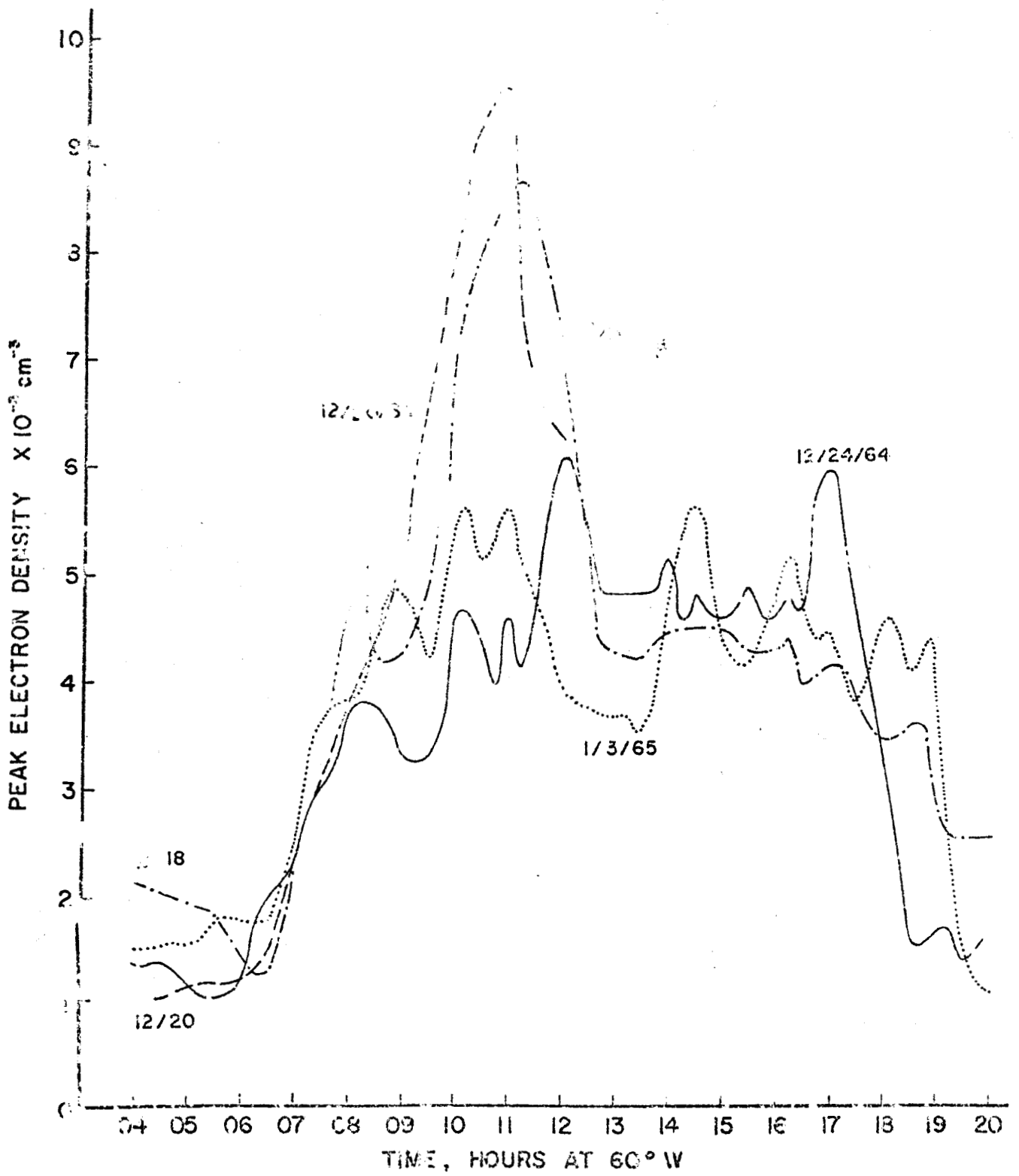
References

- Carlson, H. C., and J. S. Nisbet, (1965) "Electron Densities and Temperatures in the F-Region from Backscatter Measurements at Arecibo", Presented to the NATO Advance Study Institute on "Electron Density Profiles in the Ionosphere and Exosphere", Finse, Norway, April 1965.
- Doupnik, J. R., and E. R. Schmerling, (1965) "The Reduction of Ionograms from the Bottomside and Topside", Pennsylvania State University, Ionosphere Research Laboratory Scientific Report 230.
- Hanson, W. B., (1963) "Electron Temperatures in the Upper Atmosphere", Space Research III, John Wiley.
- Harris, I. and W. Priester, (1962) "Theoretical Models for the Solar Cycle Variation of the Upper Atmosphere", NASA Tech. Note 1444.
- Quinn, T. P. and J. S. Nisbet, (1965) "Recombination and Transport in the Nighttime F-Layer of the Ionosphere", J. Geophys. Res. 70, 113-130.
- Swider, W., (1963) "The Ionic Structure of the Ionosphere", Pennsylvania State University, Ionosphere Research Laboratory Scientific Report 201.



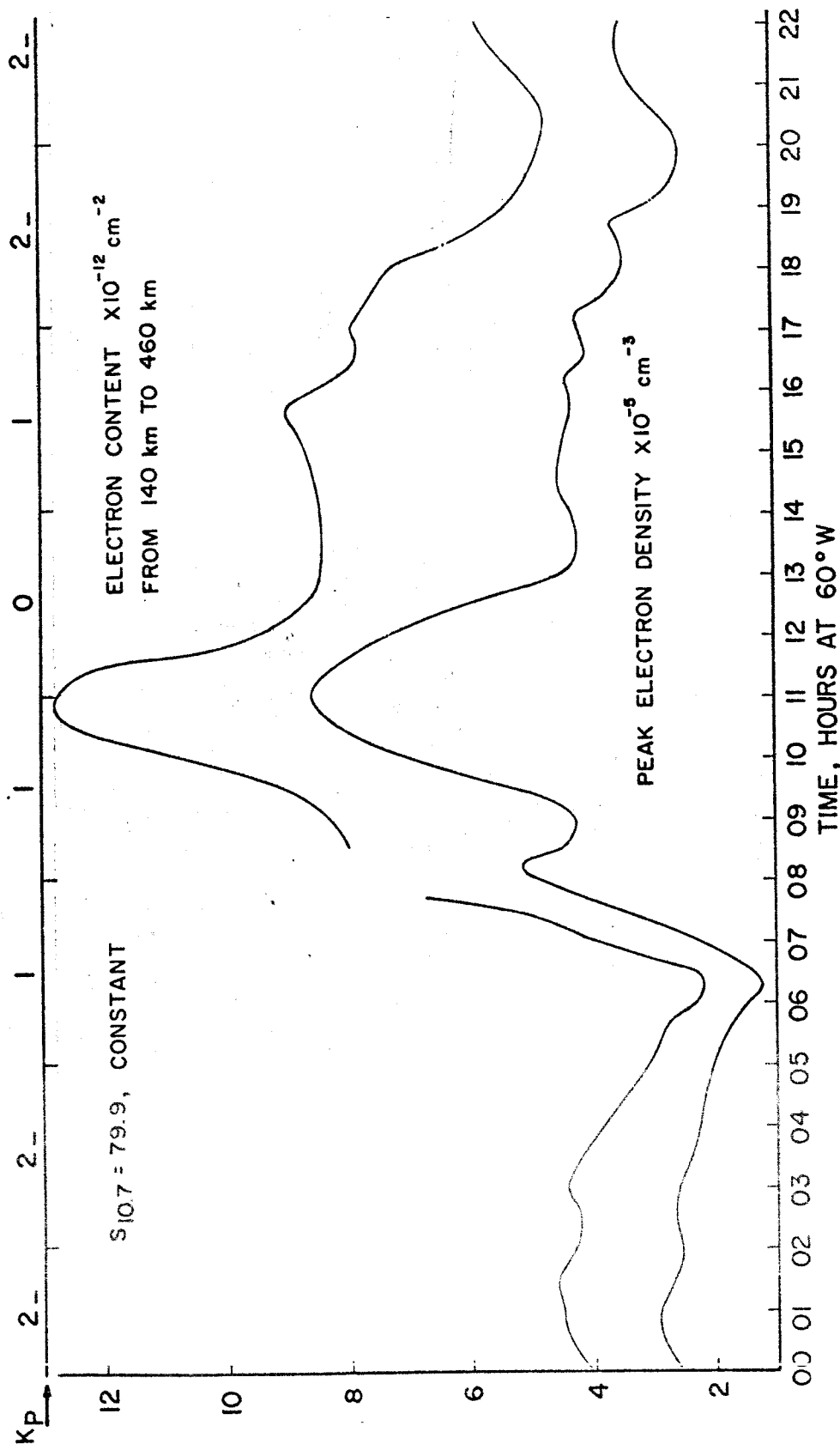
PEAK ELECTRON DENSITIES AT ARECIBO ON 12/18/64

Figure 1

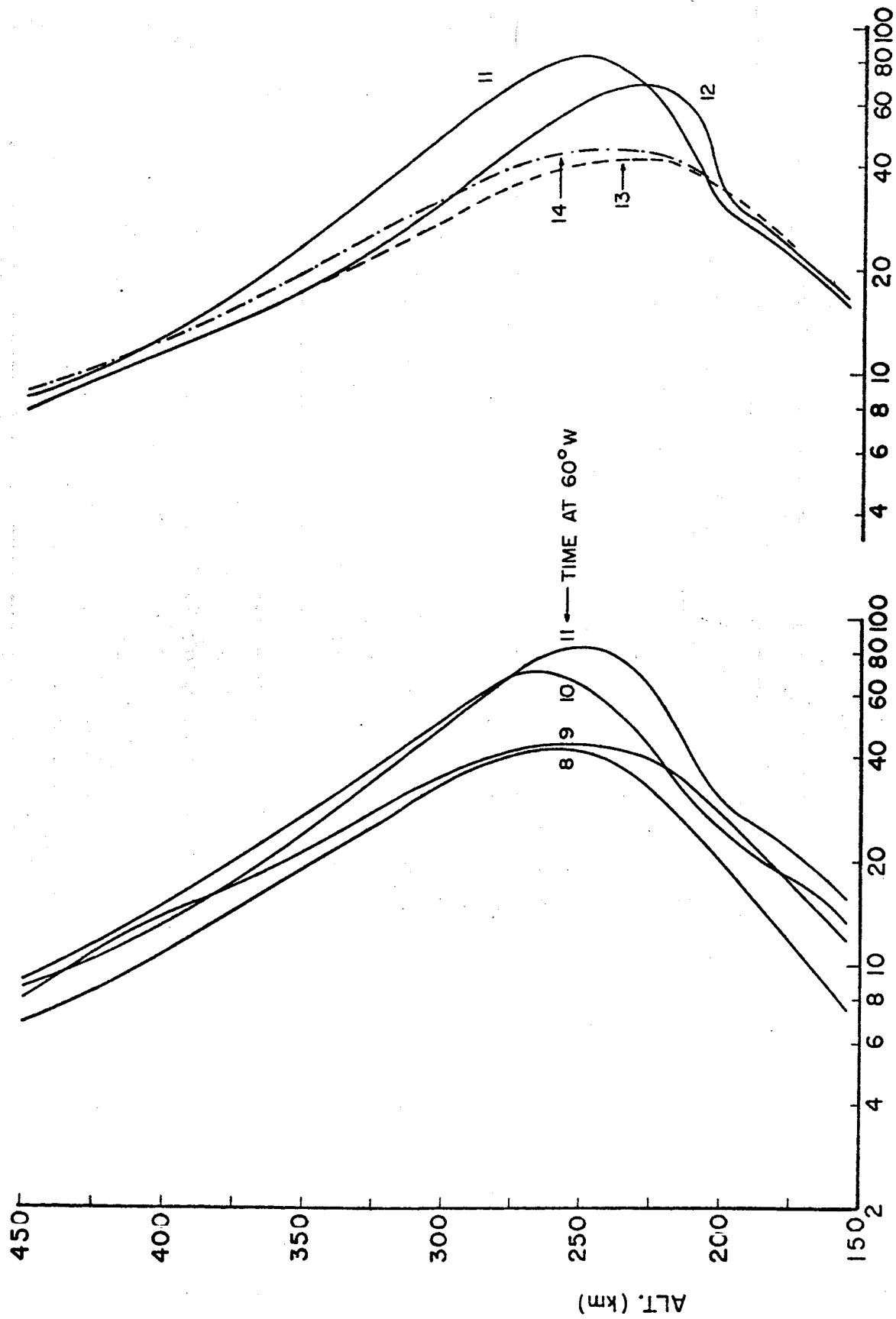


PEAK ELECTRON DENSITIES OBSERVED ON SEVERAL QUIET WINTER DAYS. DENSITIES COMPUTED FROM LOGGRAMS

Figure 2

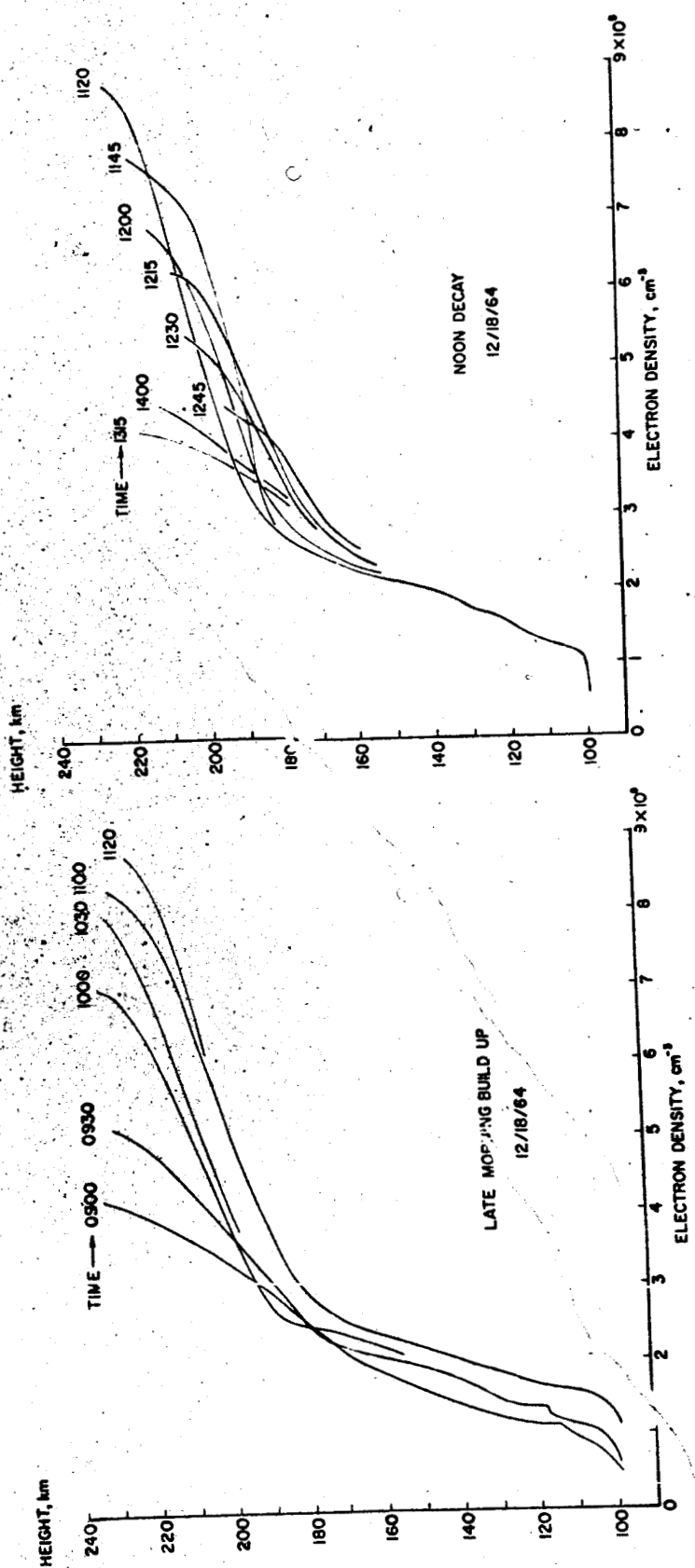


ELECTRON CONTENT COMPUTED FROM BACKSCATTER OBSERVATIONS ON 12/18/64. PEAK ELECTRON DENSITIES ARE SHOWN FOR COMPARISON. 3 HOURLY K_p INDICES AND 10.7cm SOLAR FLUX INDICATE QUIET MAGNETIC AND SOLAR CONDITIONS.



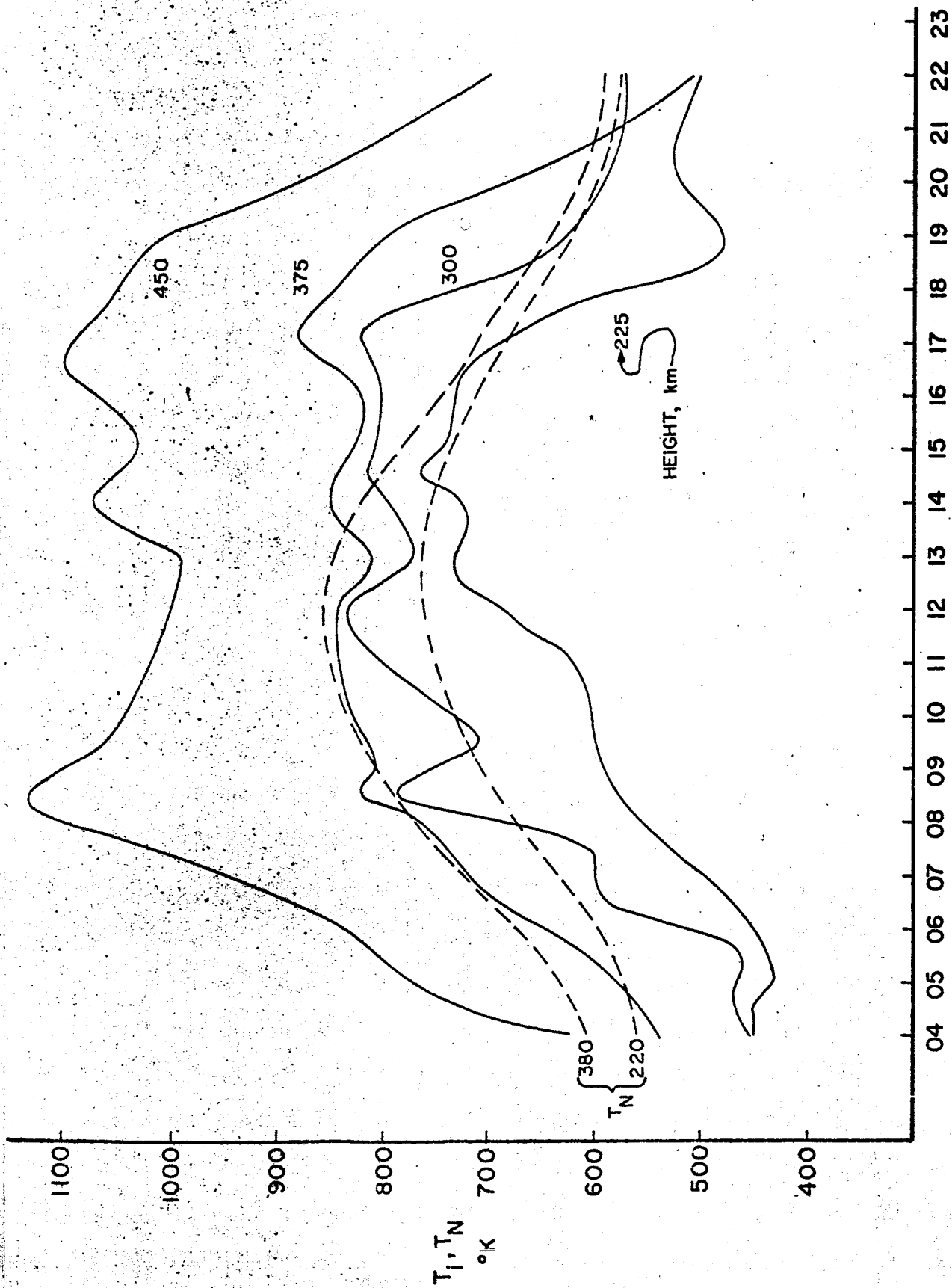
ELECTRON DENSITY PROFILES FROM BACKSCATTER MEASUREMENTS ON 12-18-64.
 SHOWING THE BUILDUP AND DECAY OF THE 11AM MAXIMUM

Figure 4



ELECTRON DENSITY TRUE HEIGHT PROFILES FROM ARECIBO IONOGRAMS. TIMES ARE FOR 60° WEST.

Figure 5



ION TEMPERATURES MEASURED ON 12/18/64. NEUTRAL TEMPERATURES WERE TAKEN FROM HARRIS AND PRIESTER'S MODEL ATMOSPHERE FOR S=70

Figure 6

$$\frac{\partial}{\partial t} \int_{140 \text{ km}}^{460 \text{ km}} N_e dZ \approx \int q dZ - \int l dZ$$

$$= Q - L$$

WHERE $Q \propto I_{\infty} \cos X$

$$L = \int \frac{\gamma_1 \gamma_2 N(N_2) N_e^2}{\gamma_1 N(N_2) + \gamma_2 N_e} dZ$$

I_{∞} IS THE UNATTENUATED SOLAR FLUX

X IS THE SOLAR ZENITH ANGLE

γ_1 $2 \times 10^{-18} \text{ cm}^3 \text{ sec}^{-1}$ (SWIDER, 1963)

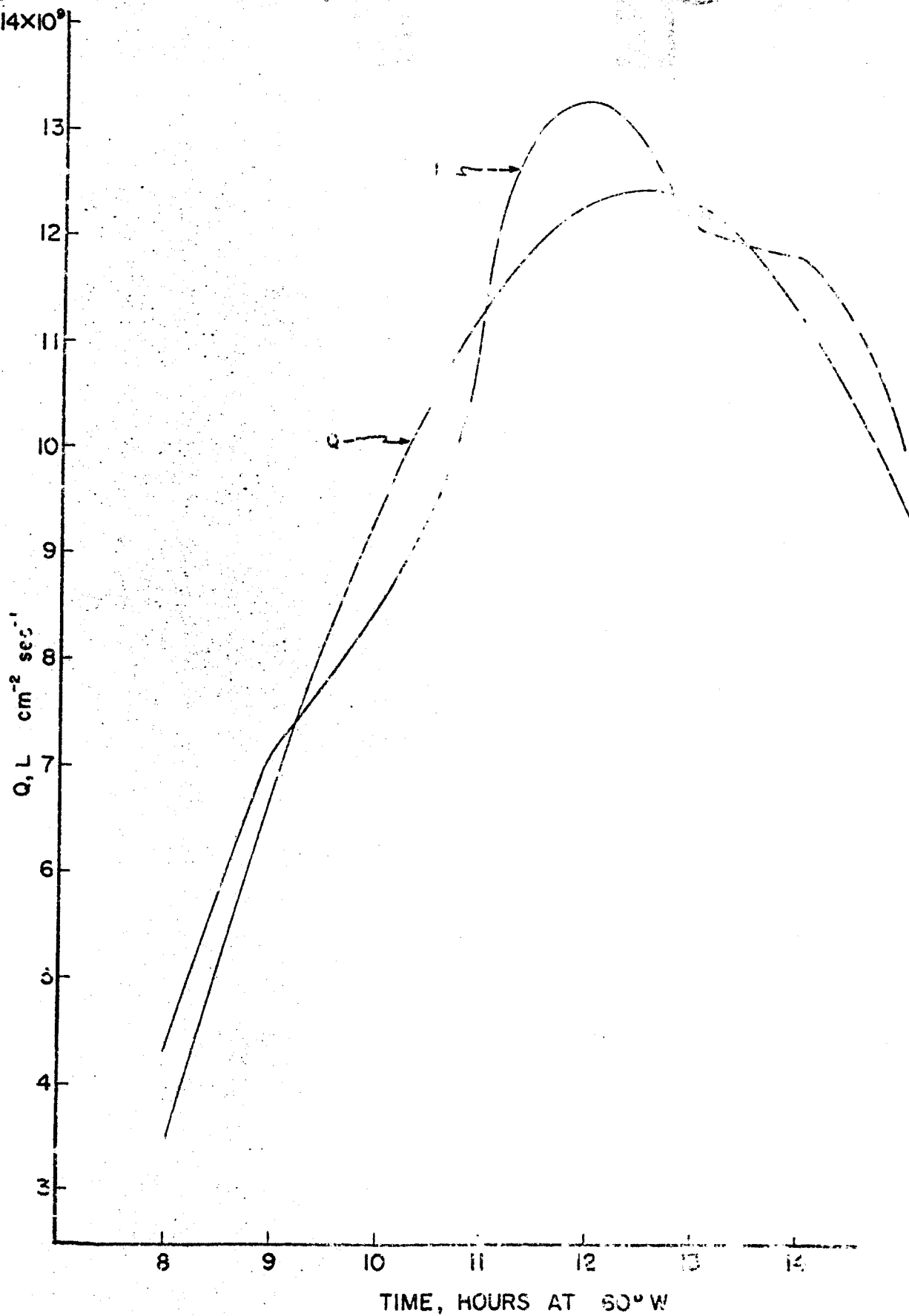
γ_2 $5 \times 10^{-9} \text{ cm}^3 \text{ sec}^{-1}$ (QUINN AND NISBET, 1965)

N_e IS THE ELECTRON DENSITY

$N(N_2)$ IS THE MOLECULAR NITROGEN DENSITY

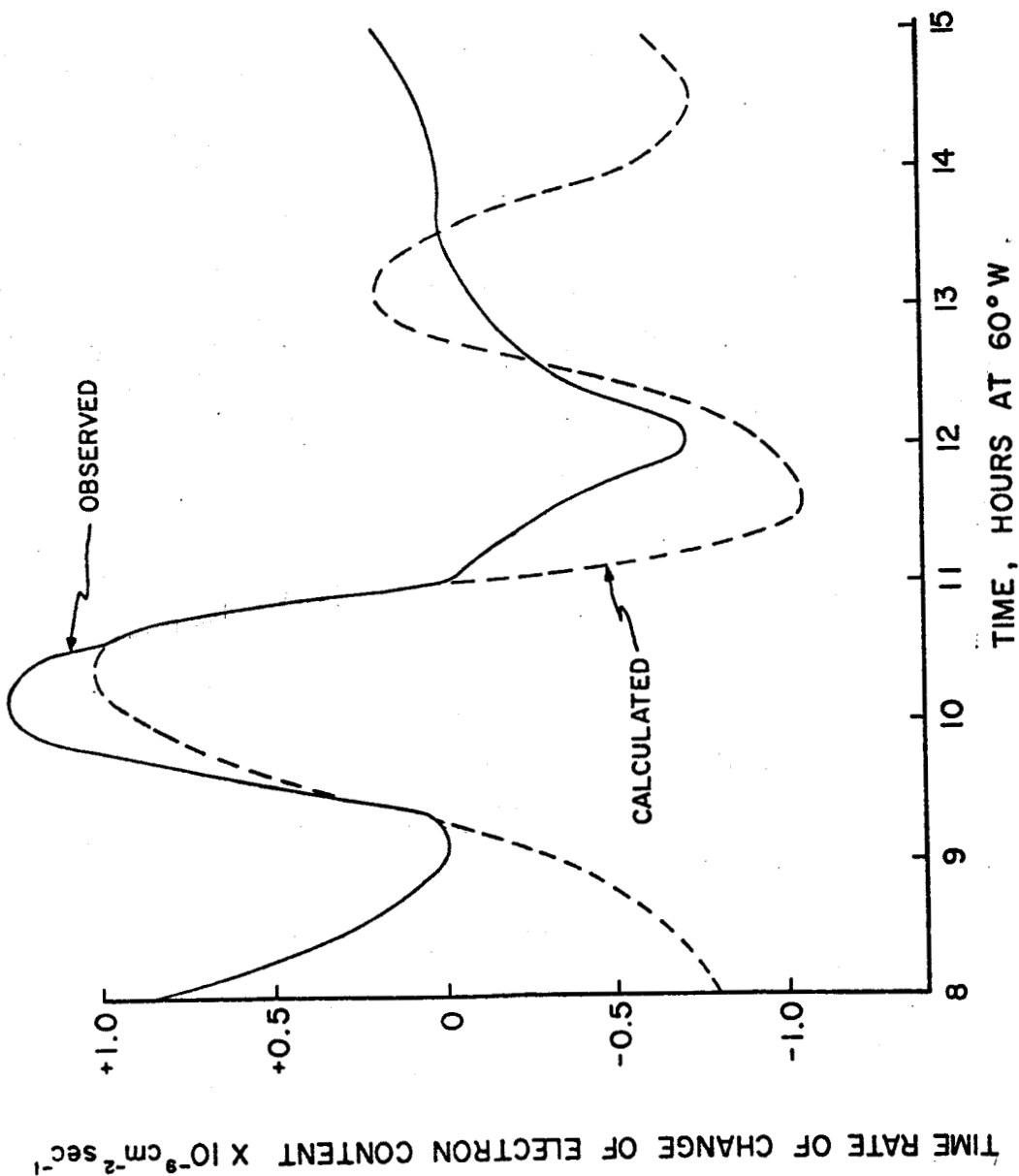
INTEGRATED CONTINUITY EQUATION. DIFFUSION FLUXES AT 140 km AND 460 km HAVE BEEN ASSUMED TO BE NEGLIGIBLE

Figure 7



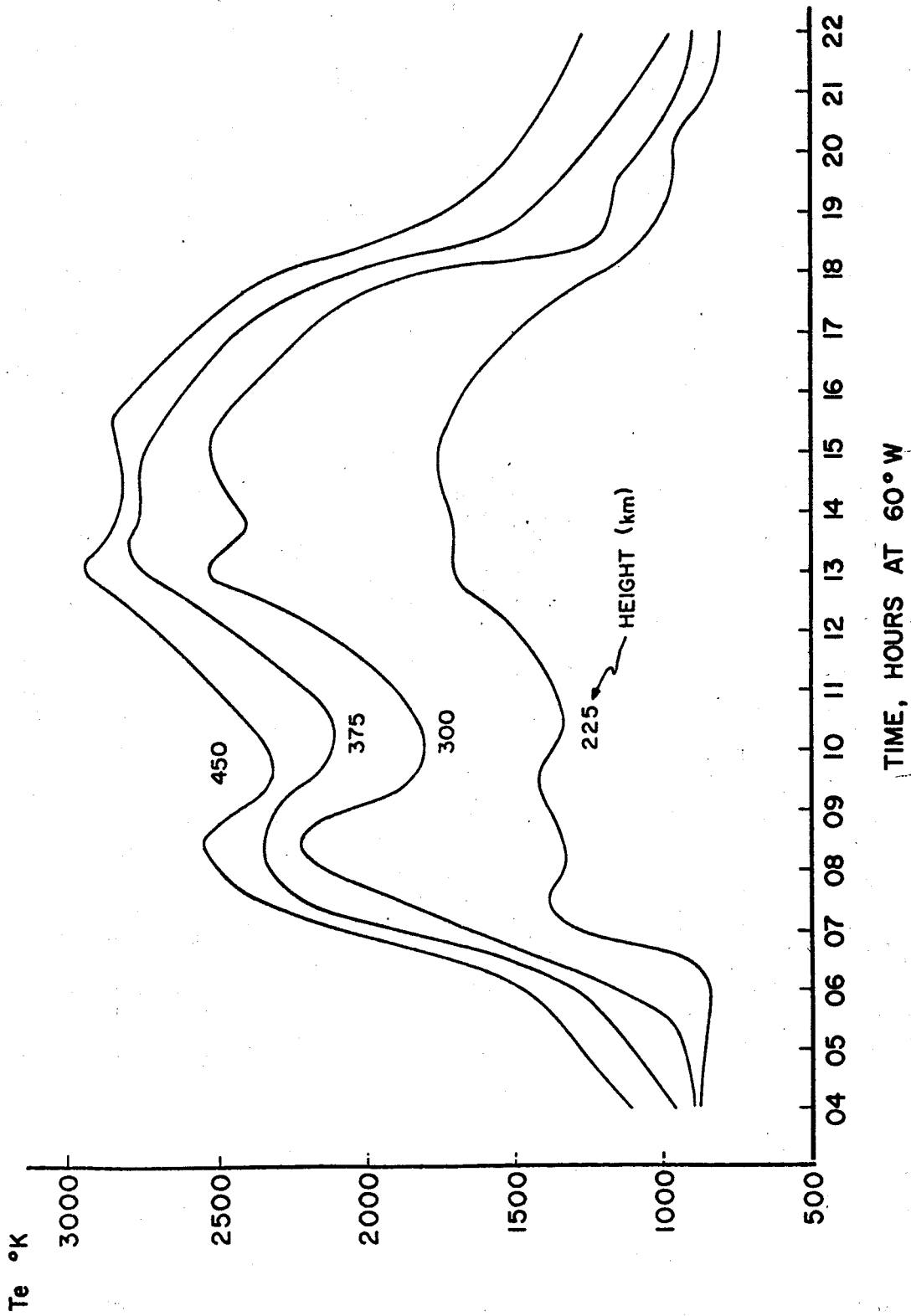
INTEGRATED PRODUCTION AND LOSS CALCULATED FOR 12°

Figure 8

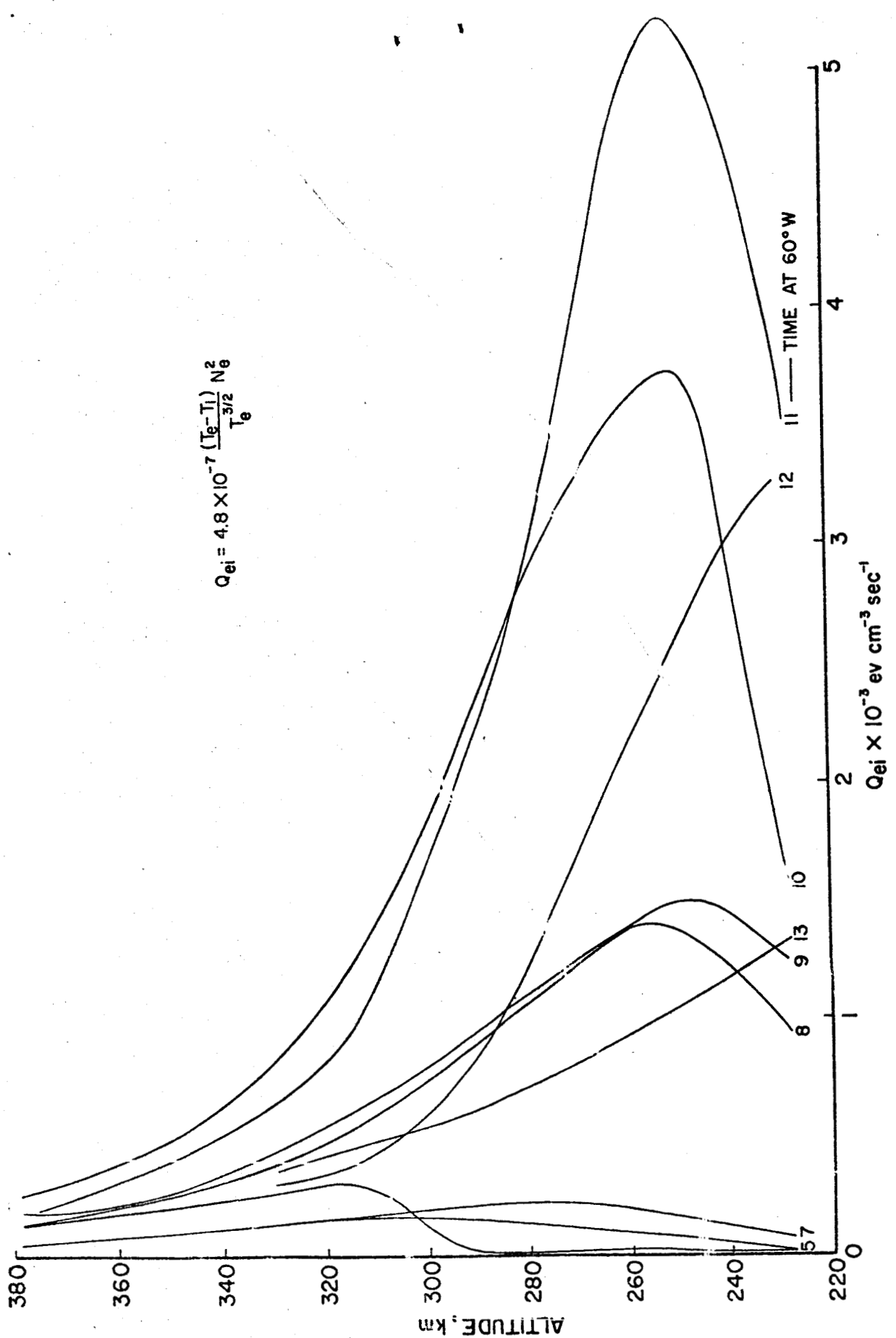


COMPARISON OF OBSERVED AND CALCULATED TIME RATES OF CHANGE OF ELECTRON CONTENT ON 12/18/64

Figure 9



ELECTRON TEMPERATURES OBSERVED ON 12/18/64



ELECTRON TO ION ENERGY LOSS RATES ON 12/18/64

Figure 11